Proceedings of the International Conference on Heat Transfer and Fluid Flow
Prague, Czech Republic, August 11-12, 2014
Paper No. 126

Design of the Capillary Pumped Loop of the Solar Thermal Storage System

Wei-Keng Li, Chien Huang, Yu-Lin Chuang
Engineering & System Science Department, National Tsing-Hua University 101,
sec.2, Kuang Fu Rd., Hsinchu, Taiwan
wklin@ess.nthu.edu.tw; bob123huang@gmail.com; rex0531@hotmail.com

Abstract - Capillary Pumped Loop (CPL) is a high-efficiency two-phase heat removal device. The heat removed method is using the phase change energy thermal energy from the working fluid of the evaporator to the condenser. The purpose of this paper is to study the possibility of the CPL apply on the solar thermal storage system. Experimental results show that the conversion efficiency of the heating of cold water is 77% higher than that of the conventional flat-plate solar water heater. In addition, when the evaporation portion has a tilt angle, the CPL system will speed up the start-up time, and result in the more uniform temperature in evaporation section. The most quick start-up time occurs on the tilt angle 90^0 when the heating power is 210W; the start-up time is 12 minutes.

Keywords**:** Solar thermal storage, CPL, Thermal convert efficiency, Phase change energy.

1. Introduction

Solar water heater is using the solar radiant heat to heat the water inside the collector plate. The hot water storage in the tank providing the necessary daily life or industrial water use, therefore, part of the energy consumed to heat the water (electric or gas) can be replaced by this device. Solar water heaters can be divided into direct heating circulation system (Kumar, Rosen 2011; Hossain et al., 2011) and indirect heating circulation system (Hussein, 2007; Chien et al., 2011; Redpath, 2012; Huang et al., 2005; Aung, Li 2013).In recent years, in order to increase the efficiency of solar thermal storage, some of the solar energy collector was improved such as V-groove shape in the thermal collector (Dua et al., 2013). To increase the thermal conductivity, some of the collector was added nanoparticles to increase the working fluid loop solar thermal storage ability or heat absorption of solar radiation (Cong et al., 2012; Lu et al., 2011). Some of the system combined with solar thermal collector plate (Taylor er al., 2011) and solar cell or thermoelectric materials (Riffat, Cuce, 2011) and obtained an extra electricity power features from the system. The purpose of this paper is combined capillary pumped loop with solar thermal storage system, which is using the evaporator of CPL to absorb the sun radiation thermal energy and carry this high temperature working fluid into the condenser of the CPL and then transfer the thermal energy into the water storage tank. CPL is a high efficiency heat transfer device using the phase change of working fluid to transport heat from evaporator to condenser; it's a cyclic circulation pumped by capillary force. Since CPL doesn't need any other mechanical force such as pump, it might be used to do the thermal management of high power electronic component on spacecraft.

In this paper, the design of solar thermal storage namely CPL has three parallel evaporators with vertically arranged from bottom to top, the evaporators were then join to a vapour line and to the condenser. The condenser was set around 50cm above the evaporator in this loop.

2. Experiment

Figure 1 is the schematic diagram of CPL solar thermal storage system, comprising Evaporator, Condenser, water tank, liquid line and the vapour line, the geometric specifications of the elements shown as in Table 1. The loop was evacuated to reduce non-condensable gases generated in the pipe line; the

vacuum degree of the loop is 10^{-4}torr. Filling ratio (V^{+}) is calculated according to the ratio of the inventory liquid volume divided by the total volume of the loop:

$$V^{+} = \frac{V_{fill}}{V_{total}} \quad (1)$$

Where V_{fill} represented the inventory liquid volume charging into the loop and V_{total} is total volume of the loop. The tilt angle (α) is defined the angle between horizontal and the liquid head, Figure 1 is the schematic diagram of loop at angleα=0^0, while Fig. 2 is the schematic diagram of loop at angle α = 45^0. Evaporator in the loop is as a heat absorbing fluid-driven elements, the structure of aluminium extrusion groove tube is inserted by a hollow porous material cylinder as shown in Figure 3a, 3b. The working fluid radial flows from the inner channel of porous tube to the recess groove which design with a ladder shape. The operation model is when the working fluid is heated in the groove, vaporize and become to vapor. The steam is then axial flow to the both end of the tube. However, the end of the liquid head is sealed that not allowing the vapor pass through, therefore, all the vapor can only pass through from the vapor head of the loop. A one way flow direction is hence occurred in the loop. Fig. 4 is the shape of the condenser, made by a copper tube immersed into a 9 litter cooling water tank. The water temperature in water tank is 25C for example, by the time when the steam flow in, the temperature is gradually increased, so that make the CPL loop has a heater function. Solar water heaters is the use of solar thermal energy to heat water, but the real test cannot effectively simulate the sun's radiant energy, and that is a really problem for the calculation of the thermal energy conversion efficiency. Therefore, in this experiment, we use the electric heating instead of the sunlight irradiation. The way we do is using the power supply to provide a certain input voltage and current and that will be able to calculate heating power. The heater is a copper block with a heat rod inserted inside the block, and was placed on the surface of the evaporator (Fig. 3a). Methanol is chosen as the working liquid in this study. The system consists of nine T-type thermocouples, and all temperature sensors are connected with a programmable controller (PLC) to record temperature changes. Tv1, Tv2 and Tv3 represent the vapor head temperature on the evaporator (I), evaporator (II) and evaporator (III) respectively while TL1, TL2 and TL3 represent the liquid head temperature on the evaporator (I), evaporator (II) and evaporator (III) respectively. Tc in behalf of the condenser inlet temperature; $T_{w,up}$ and $T_{w,down}$ represent the upper and lower barrel storage temperature, the distance from $T_{w,up}$ to $T_{w,down}$ is about 150mm, while the height of $T_{w,down}$ is 100mm measuring from the bottom of the reservoir tank. The whole loop is well insulated with an insulation foam material.

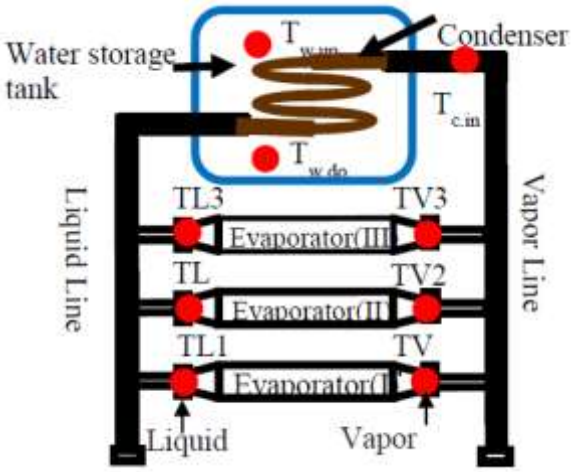

Fig.1. Schematic diagrams of the loop and temperature measurements points at angle α = 0^0

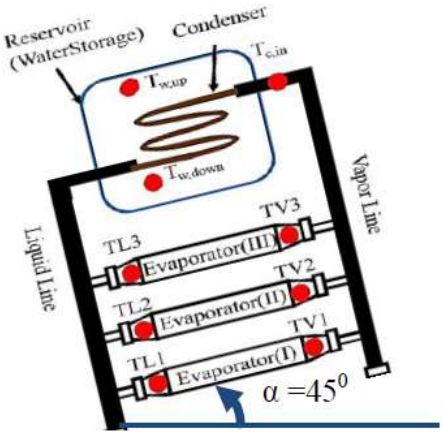

Fig.2. schematic diagram of loop at angle α = 450.

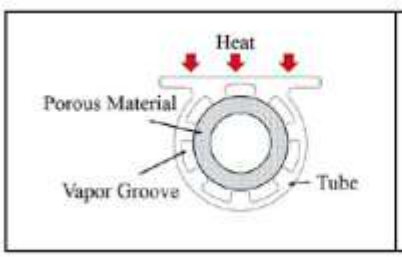

Fig. 3a. Section of the evaporator

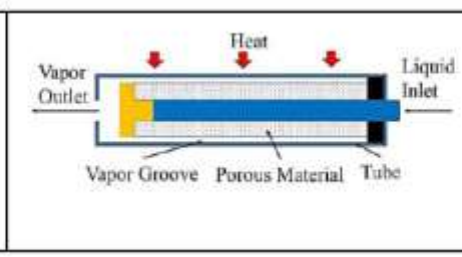

Fig. 3b. Axial direction

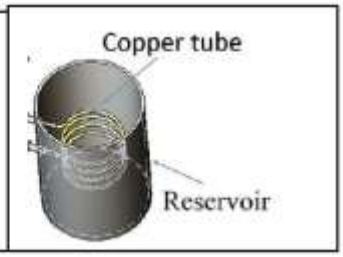

Fig. 4. Shape of the condenser

Table 1. Geometric specifications of the CPL solar thermal storage elements.

Element	Volume cm^3	Outside diameter mm	Inner diameter mm	Length mm	Width mm
Evaporator	V_E= 270	$O.D._E$=19	$I.D._E$=13.5	L_E=430*3	
Condenser	V_C=75	$O.D._C$=5.35	$I.D._C$=6.35	L_C=180	
Reservoir	V_{Res}=10000	$O.D._{Res}$=214	$I.D._{Res}$=200		
Liquid Line	V_{LL}=255	$O.D._{LL}$=20.5	$I.D._{LL}$=18.5	L_{LL}=950	
Vapor Line	V_{VL}=120	$O.D._{VL}$=20.5	$I.D._{VL}$=18.5	L_{VL}=450	
heater	V_H=135			L_H=300	W_H=15

3. Results and Discussion

3.1. Start-Up Experiment at Constant Power 210W but Different Working Fluid Inventory at $\alpha = 0^0$

This paper defines the start-up time is after the loop start of heating, the time required when the $T_{c,in}$ temperature reach to the peak point. When the temperature $T_{c,in}$ to the maximum value, the steam starts to flow from evaporator to condenser and heat exchange starts to occurs at that time. Figure 5 is $T_{c,in}$ distribution at a heating power 210W (single power 70W). In this experiment, the initial value of $T_{c,in}$ is about 22 ℃, when the vapor be push flows from evaporator into condenser, the condensing inlet temperature is gradually increased, resulting in a peak-value, and finally reach to steady state.

Figure 6 is the trend of start-up time with respect to peak temperature $T_{c,in}$ at tilt angle ($\alpha = 0^0$) and power (210 W). The higher of the temperature $T_{c,in}$ represented the longer of the heating time. Generally, the lower the filling ratio has less start-up time (when 65% of start-up time is 14 minutes), and a higher filling ratio requires a longer start-up time (when 85% of start-up time is 22 minutes), it is also implying that a high filling ratio requires a larger vapor pressure to make the fluid circulated within the loop.

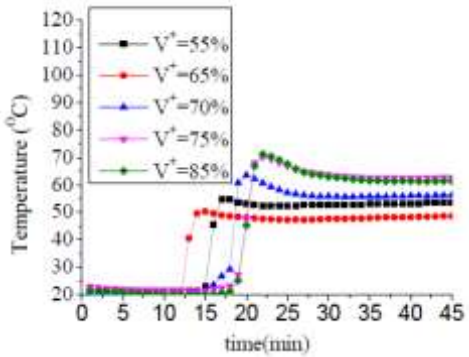

Fig.5.$T_{c,in}$ temperature distribution at $\alpha=0^0$ and power 210W

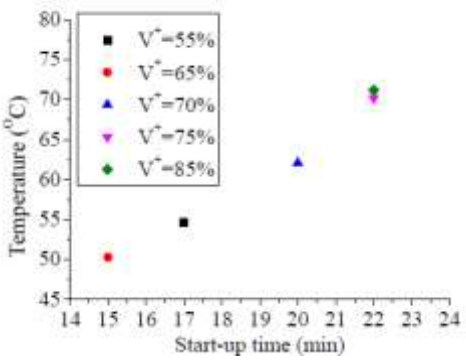

Fig.6. Trend of the start-up time with respect to the peak temperature $T_{c,in}$ at the tilt angle ($\alpha = 0^0$) and power (210 W)

3.2 Evaporator Temperature Distribution at Constant Total Power 210W and $\alpha=0^0$ but Different Working Fluid Inventory

Figure 7 is evaporator temperature distribution at power 210W and filling ratio 85%. When the loop was began to heat and with the time increasing, the evaporator temperature is increasing as well. Vapor generated from the evaporator is then flow into the vapor head, therefore, result in the vapor head temperature (TV1, TV2, TV3) and liquid head temperature (TL1, TL2, TL3) are on the rise. Due to the structure of the evaporator, the flow is one way direction and makes the most of the vapor will flow from the vapor head to the vapor line and finally to the condenser. When the temperature of the working fluid in the system reaches operating temperature, the loop started. With the heat of condensation of the vapor start to promote circulation of the working fluid in the loop, the low temperature liquid is flowing through the liquid head back to the evaporator, hence makes the temperature of the evaporator decreased until the steady state is reached. in figure 7, the vapor head temperature TV3 is larger than TV2 and TV1, that is because the evaporator are sequentially arrange from the upper TV3 and then TV2 and finally to the bottom TV1. Therefore, vapor is flowing from the evaporator (I) to evaporator (II) and evaporator (III) that will result in the temperature of the vapor head at evaporator (I) be the lowest while vapor head evaporator (III) be the highest. It is also implying the temperature of vapor head (III) will be much impacted by the other two vapor heads. The similar situation will happen on the liquid head for the liquid head temperature (TL3) is larger than the liquid head temperature TL2 and TL1.

Figure 8 is the evaporator temperature distribution at power 210W (75%) and $\alpha = 0$. Compare figure 7 (85%) and figure 8 (75%), both of the evaporator temperature distributions are very similar, which shows the filling ratio in this range is quite stable, however, the temperature of TV3 is up to 95 ℃, which is the relative disadvantage of the loop.

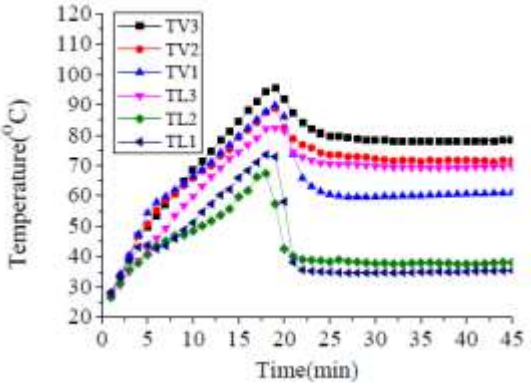

Fig. 7. Evaporator temperature distribution at power 210W with filling ratio (V^+=85%) and $\alpha=0^0$

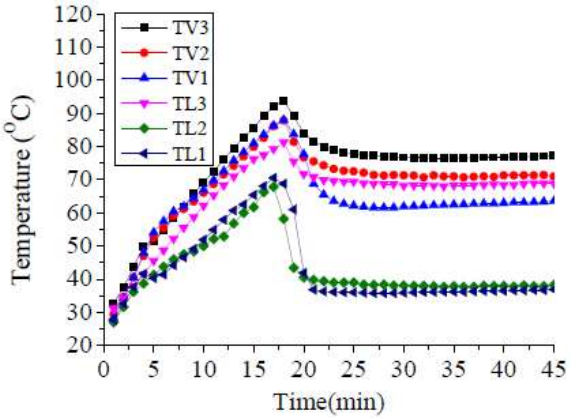

Fig. 8. Evaporator temperature distribution at power 210W with filling ratio (V+=75%) and $\alpha=0^0$

Fig. 9 is evaporator temperature distribution at power 210W with filling ratio (V^+=70%) and $\alpha=0^0$. From the figure, the trend between TL3 and TV3 almost identical, except the vapor back flush cause the temperature of TL3 rises. In this test, when the filling amount is too less that will cause the condensed liquid back flow to the evaporator (III) reduced, which will result in the increasing of the liquid head temperature TL3. Evaporator temperature of the inventory at 70% is lower than that of the inventory at 85%, shows a high filling ratio need a greater vapor pressure to overcome the gravity and make the loop circulate smoothly. That is why the evaporator temperature at inventory V^+ = 85% is higher than that of the temperature at inventory V^+ = 70%.

Fig. 10 is evaporator temperature distribution at power 210W with filling ratio (V+=65%) and α=00. In this test, the evaporator temperature (III) keeping raising that is because the less amount of the working fluid can't condensed a sufficient liquid flow into the evaporator and thus result in the dry out of the

evaporator (III).

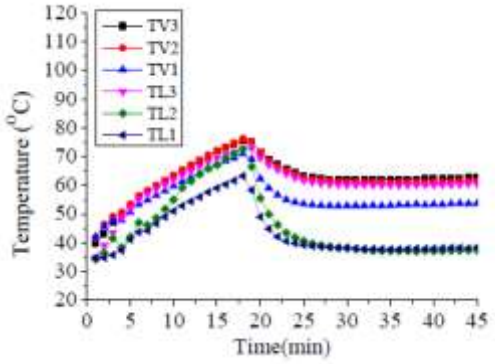

Fig. 9. Evaporator temperature distribution at power 210W with filling ratio (V+=70%) and α=00

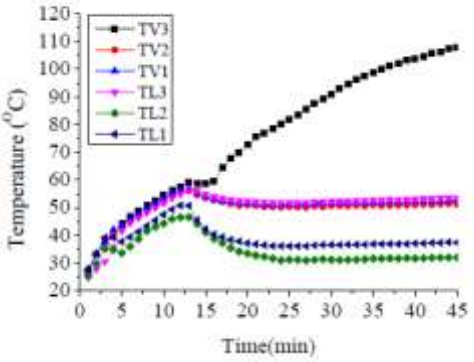

Fig. 10 is evaporator temperature distribution at power 210W with filling ratio (V^{+}=65%) and $\alpha=0^{0}$.

Figure 11 is evaporator temperature distribution at power 210W with filling ratio (V^{+}=55%) and $\alpha=0^{0}$. Due to lower filling ratio in this test, not only TV3 unable to reach steady state, TL3 can't reach a steady state as well, the dry out phenomena seems more serious in this situation. Based on the above discussion, the filling amount of the working fluid has a considerable influence on the operation of the CPL solar thermal heater. Therefore, the shortage of the working fluid filling will cause evaporator easy dry out, and making the loop can't be stable operation; on the contrary, the excess of the filling ratio will cause blockage in the loop and making the loop requires a large vapor pressure. Therefore, it is very important to find an optimal filling ratio to obtain maximum thermal convert efficiency and enable loop stable operation. In this paper, the thermal convert efficiency (η_{th}) shown as in Eq. (2), is defined as thermal stored energy of the storage tank ($Q_{reservoir}$) divided by the power supply (Q_{in}). $Q_{reservoir}$ shown as in Eq. (3), is thermal energy of the storage tank. Total input thermal energy is the power input times the time interval between t_1 and t_2 shown as in Eq. (4). All the symbols are described in Table 2.

$$\eta_{th} = \frac{Q_{reservoir}}{Q_{in}} \times 100\% \tag{2}$$

$$Q_{reservoir} = mC_p(T_{w,t2} - T_{w,t1}) \tag{3}$$

$$Q_{in} = P_{total} \times (t_2 - t_1) \tag{4}$$

Table 2. Nomenclature of the CPL solar thermal storage loop.

Symbol	Description	Symbol	Description
η_{th}	thermal convert efficiency	$T_{W,up,t1}$	$T_{W,up}$ temperature at time t_1 (℃)
t_1	loop start up time (s)	$T_{W,up,t2}$	$T_{W,up}$ temperature at time t_2 (℃)
t_2	Half an hour after the loop start (s)	$T_{w,down,t1}$	$T_{w,down}$ temperature at time t_1 (℃)
C_p	Heat capacity of water (J/g.K)	$T_{w,down,t2}$	$T_{w,down}$ temperature at time t_2 (℃)
m	The water quantity in the storage tank (g)	P_{tot}	Power supply (W)
$T_{w,t1}=(T_{W,up,t1} + T_{w,down,t1})/2$	The average temperature of the water tank at initial time t_1 (℃)	Q_{in}	Total input thermal energy (J)
$T_{w,t2}=(T_{W,up,t2} + T_{w,down,t2})/2$	The average temperature of the water storage tank at time t_2 (℃)	$Q_{reservoir}$	Thermal energy of the storage tank (J)

Figure 12 shows the relationship between the filling ratio with respect to the thermal convert efficiency at 210W and α=0, the maximum convert efficiency is 77% (V + = 70%). At low filling ratio (55%, 65%), the insufficient condensed liquid can't flow into the evaporator in time, and thus causing the dry out happens. At high filling ratio (75%, 80%), it need high vapor pressure to push the loop operation, and that will cause thermal convert efficient decreased. Therefore, figure 12 shows the filling ratio has a significant influence on the loop performance

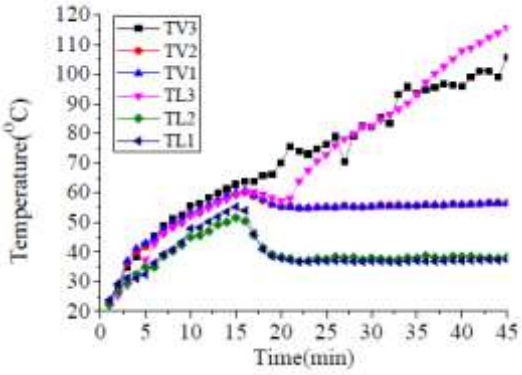

Fig. 11. Evaporator temperature distribution at power 210W with filling ratio (V^{+}=55%) and $\alpha=0^{0}$

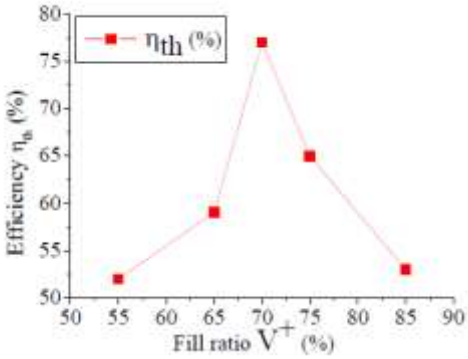

Fig. 12. Effect of the filling ratio with respect to thermal convert efficiency at 210W and $\alpha=0^{0}$

3.3 Heat Loading Sharing Experiment of the CPL Solar Thermal Storage System

Heat loading sharing experiment means when one of the evaporator is heating while the other two are not. In this case, the evaporator without heating may become the heat sink of the evaporators that was heating. Fig. 13 is the evaporator temperature distribution for the heat loading sharing experiment at power input 70W on evaporator (III), V^{+}=70%, $\alpha=0^{0}$. In this case, TV3 and TL3 will rise and reach to steady state, the position of evaporator (III) is higher than that of the other two evaporators, therefore, vapor from the evaporation (III) will not flow down to the (II) and (I) unit but directly flow upward by the buoyancy force and into the vapor line. In the meantime, due to the heat conduction through the tube wall, TV2 and TL2 will also slowly rise. Fig. 14 is the evaporator temperature distribution for the heat loading sharing experiment at power input 70W on evaporator (II) with V^{+}=70% and $\alpha=0^{0}$. Similar with figure 13, TV2 are the first one of temperature rising. However, due to the reason of the buoyancy force, the vapor out of the evaporator (II) could flow into the evaporator (III), thus also makes TV3 and TL3 temperature rising. In the meantime, due to the heat conduction, evaporator (I) temperature will also slowly rise.

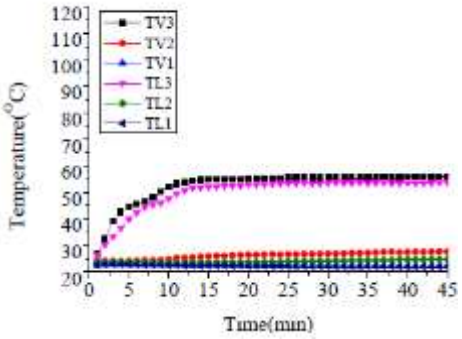

Fig. 13. Evaporator temperature distribution for the heat loading sharing experiment at power input 70W on evaporator (III) with V+=70% and α=00

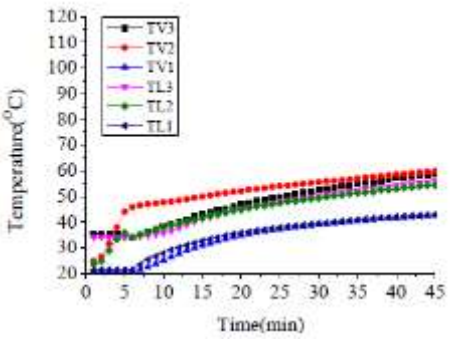

Fig. 14. Evaporator temperature distribution for the heat loading sharing experiment at power input 70W on evaporator (II) with V+=70% and α=00

Figure 15 is evaporator temperature distribution for heat loading sharing experiment at power input 70W on evaporator (I) with V+=70% and α=0. The Figure shows the temperature for the evaporator (I), evaporator (II) and evaporator (III) were increased. It is also implying that the heat was transfer from evaporator (I) to evaporator (II) and evaporation (III). Comparison TV3 and TV2, although the distance between evaporator (III) and evaporator(I) is much longer than that of the distance between evaporator (II) and evaporator (I), however, the temperature of TV3 rising earlier than TV2, that is because the high temperature vapor from the evaporation (I) was directly upward flow to the evaporation (III).

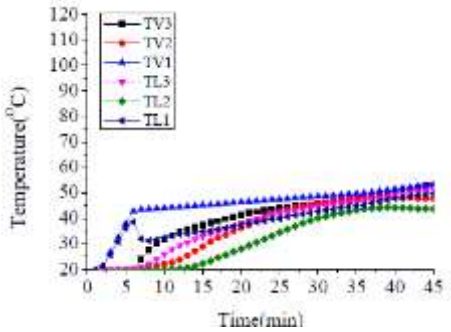

Fig. 15. Evaporator temperature distribution for the heat loading sharing experiment at power input 70W on evaporator (I) with V^{+}=70% and $\alpha=0^{0}$

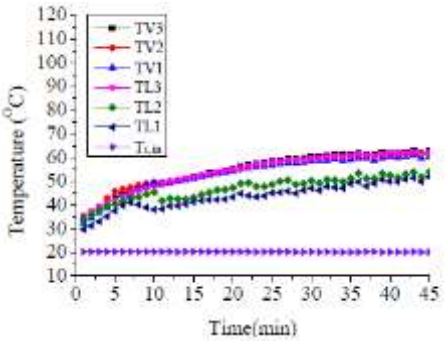

Fig. 16. Evaporator temperature distribution for low total power 90W (30W/evaporator) at V^{+}=70% and $\alpha=0^{0}$

3.4 Start-up Experiment with Different Power but Constant Working Fluid Inventory 70% at $\alpha=0^{0}$

Figure 16 shows the temperature distribution at low power 90W (30W/evaporator), in this case, the loop does not start because the inlet temperature of the condenser $T_{c,in}$ did not rise, which means that the vapor pressure of 90W power generated from evaporators is not sufficient to start up the circulation of working fluid within the loop.

Fig. 17 is evaporator temperature distribution for low total power 150W (50W/evaporator) at V^{+}=70% and $\alpha=0^{0}$. The temperature of the evaporator is fluctuated and it also proved the status of the loop never reach to steady state in this low power case.

Fig. 18 is evaporator temperature distribution for low total power 270W (90W/evaporator) at V^{+}=70% and $\alpha=0^{0}$, the evaporator temperature rises very rapidly, and finally reach to a steady state in this case. Comparison of figure 9 (210W) and figure 18 (270W), the evaporator temperature distribution are similar except the steady state evaporator temperature TV3 in power 270W (Tv3=75°C) is higher than that of the evaporator temperature in power 210W (Tv3=65°C).

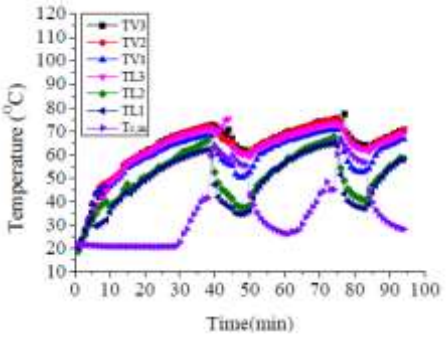

Fig. 17. Evaporator temperature distribution for low total power 150W (50W/evaporator) at V^{+}=70% and $\alpha=0^{0}$

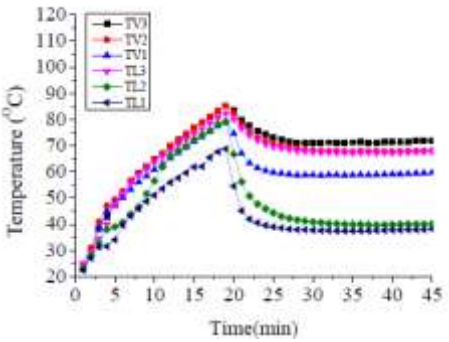

Fig. 18. Evaporator temperature distribution for low total power 270W (90W/evaporator) at V^{+}=70% and $\alpha=0^{0}$

Fig. 19 is evaporator temperature distribution for low total power 150W (50W/evaporator) at

V^+=70% and $\alpha=0^0$, Under this high power test condition,TV3 temperature is all the way fluctuated and can't reach to a steady state however, both TL3 and TV3 temperatures are suddenly increasing after 35 minutes. This is because the high power input enhance the boiling mechanism in the evaporator, if the condensed liquid can't makeup to the evaporator in time, the vapor occupied in the evaporator is gradually increased, that is why TV3 temperature is higher than the others when the loop is start. As the heating time increase, the liquid head temperature TL3 is also began to rise after 35 minutes.

Figure 20 is the relationship between thermal convert efficiency and the start-up time of the loop. The figure shows the thermal convert efficiency would increase with increasing of the power input, the situation would keep this trend until the efficiency reach to a maximum at a certain power input and then start to decrease. In addition, from the figure, one may obviously observed that the loop start-up time will decrease with increasing of the power input that is because the higher power input will make the working fluid reach to the start-up temperature easily.

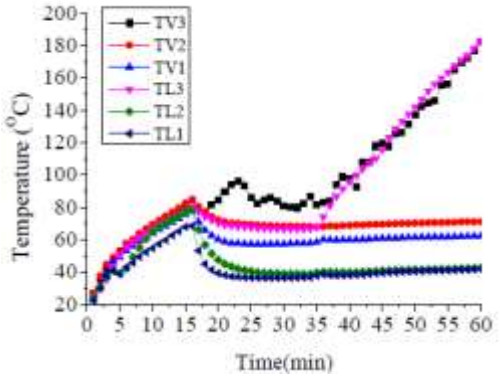

Fig. 19. Evaporator temperature distribution for low total power 150W (50W/evaporator) at V^+=70% and $\alpha=0^0$

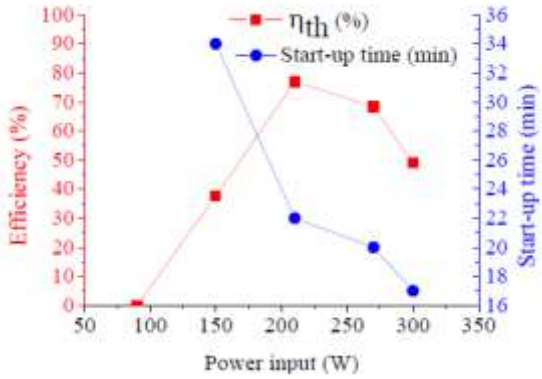

Fig. 20. Relationship between thermal convert efficiency and the start-up time of the loop

4. Conclusion

This study analyse the thermal convert efficiency of CPL solar thermal storage system in different power, tilt angle, filling ratio and start up time.

4.1 The optimal filling ratio is 70% in this study

4.2 the maximum thermal convert efficiency is 77% at the power 210W and filling ratio 70% and tilt angle $\alpha=0^0$ in this system.

4.3 The heating power has certain limits for a stable operation of the CPL solar water heaters. In this solar thermal system, the heating power must be in the range of 150W to 300W.

Acknowledgements

This project is supported by National Science Council, Taiwan, NSC-103-2623-E-007-008-ET. We acknowledge NSC for their support for this project.

References

Aung, N. Z., S. Li, (2013) "Numerical investigation on effect of riser diameter and inclination on system parameters in a two-phase closed loop thermosyphon solar water heater", Energy Conversion and Management 75 25–35.

Chien, C.C., C.K. Kung, C.C. Chang, W.S. Lee, C.S. Jwo, S.L. Chen, (2011) "Theoretical and experimental investigations of a two-phase thermosyphon solar water heater", Energy 36 415-423.

Chong, K. K., K. G. Chay, K. H. Chin, (2012) "Study of a solar water heater using stationary V-trough collector" Renewable Energy 39 207-215.

Dua, B., E. Hub, M. Kolhe, (2013) Renewable and Sustainable Energy Reviews 17119–125.

Hossain, M.S., R. Saidur , H. Fayaz, N.A. Rahim, M.R. Islam, J.U. Ahamed, M.M. Rahman, (2011) "Review on solar water heart collector and thermal energy performance of circulating pipe", Renewable and Sustainable Energy Reviews 15 3801–3812

Huang, B.J. , J.P. Lee, J.P. Chyng, (2005) "Heat-pipe enhanved solar-assisted heat pump water heater" Solar Energy 78 375–381.

Hussein, H.M.S. (2007) "Theoretical and experimental investigation of wickless heat pipes flat plate solar collector with cross flow heat exchanger"Energy Conversion and Management 48 1266–1272

Kumar, R., M. A. Rosen, (2011) "Integrated collector-storage solar water heater with extended storage unit" Applied Thermal Engineering 31, 348-354.

Lu, L., Z. H. Liu, H. S. Xiao, (2011) "Thermal performance of an open thermosyphon using nanofluids for high-temperature evacuated tubular solar collevtors: part 1: indoor experiment" Solar Energy 85 379–387.

Redpath, D. A.G. (2012) "Thermosyphon heat-pipe evacuated tube solar water heater northern maritime climates", Solar Energy 86 705–715.

Riffat1, S. B., E. Cuce, (2011) "A review on hybrid photovoltaic/thermal collectors and sysmtes" International Journal of Low-Carbon Technologies, 6 212–241.

Taylor, R., S. Coulombe, Todd Otanicar, Patrick Phelan, Andrey Gunawan, Wei Lv, Gary Rosengarten, Ravi Prasher, Himanshu Tyagi, (2013) "Small particles, big impacts: a review of the diverse applications of nanofuids" Journal Of Applied Physics 113 011301.